The Limitations of an Exclusively Colloidal View of Protein Solution Hydrodynamics and Rheology

Prasad S. Sarangapani,[†] Steven D. Hudson,[‡] Kalman B. Migler,[‡] and Jai A. Pathak[†*]

[†]Formulation Sciences Department, MedImmune, Gaithersburg, Maryland; and [‡]Materials Science and Engineering Division, National Institute of Standards and Technology, Gaithersburg, Maryland

ABSTRACT   Proteins are complex macromolecules with dynamic conformations. They are charged like colloids, but unlike colloids, charge is heterogeneously distributed on their surfaces. Here we overturn entrenched doctrine that uncritically treats bovine serum albumin (BSA) as a colloidal hard sphere by elucidating the complex pH and surface hydration-dependence of solution viscosity. We measure the infinite shear viscosity of buffered BSA solutions in a parameter space chosen to tune competing long-range repulsions and short-range attractions (2 mg/mL $\leq$ [BSA] $\leq$ 500 mg/mL and 3.0 $\leq$ pH $\leq$ 7.4). We account for surface hydration through partial specific volume to define volume fraction and determine that the pH-dependent BSA intrinsic viscosity never equals the classical hard sphere result (2.5). We attempt to fit our data to the colloidal rheology models of Russel, Saville, and Schowalter (RSS) and Krieger-Dougherty (KD), which are each routinely and successfully applied to uniformly charged suspensions and to hard-sphere suspensions, respectively. We discover that the RSS model accurately describes our data at pH 3.0, 4.0, and 5.0, but fails at pH 6.0 and 7.4, due to steeply rising solution viscosity at high concentration. When we implement the KD model with the maximum packing volume fraction as the sole floating parameter while holding the intrinsic viscosity constant, we conclude that the model only succeeds at pH 6.0 and 7.4. These findings lead us to define a minimal framework for models of crowded protein solution viscosity wherein critical protein-specific attributes (namely, conformation, surface hydration, and surface charge distribution) are addressed.

INTRODUCTION

Molecularly crowded protein solutions ubiquitously span nature and biotechnology, ranging from macromolecular crowding in cells to therapeutic protein (e.g., monoclonal antibody) solutions (1–6). They represent a frontier of soft condensed matter physics. They are complex systems with diverse intermolecular forces and many-body interactions that cannot be simplified to a single body problem because interactions at high concentrations are coupled to orientational degrees of freedom. Although intracellular proteins typically exist at concentrations up to 400 mg/mL (1,2), therapeutic antibodies are often formulated at high concentrations exceeding 100 mg/mL for parenteral subcutaneous administration. High formulation concentration is driven by the limited volume that can be administered subcutaneously as well as the high-dosing regimens (≈ 2 mg protein/Kg patient body mass) that are required, given typical potency (5–10). Because proteins have dual macromolecular and colloidal characteristics (1–4), the interplay between viscosity and stability of highly concentrated protein solutions is a concern due to changes in molecular conformation that may drive nonnative aggregation under quiescent conditions and in common unit operations, e.g., purification and filling (5–8). Concentrated protein solutions show an enhanced tendency to aggregate, which results in increased system viscosity (6–10). Understanding the physical underpinnings of the concentration-dependence of

protein solution viscosity is of fundamental importance to the bio-pharmaceutical industry, especially for therapeutic protein purification and concentration, and for facile delivery of concentrated protein therapeutic formulations.

We started this exercise with bovine serum albumin (BSA), a single-domain protein. Multidomain proteins such as immunoglobulins (IgGs) have nonnegligible interdomain interactions (11) requiring careful analysis; data on IgGs will be reported in a subsequent publication currently in preparation. Serum albumins are abundant at a concentration of 40 mg/mL in blood plasma and are responsible for a host of biological functions (12) including transporting drugs and hormones and maintaining blood pH at 7.4, where the protein possesses net charge (Z). Although $Z = 0$ at the BSA iso-electric point, pI (pH = 4.95), BSA still retains surface patches of positive (*blue*) and negative (*red*) charge (Fig. 1). While colloidal models are thought to assume uniform point charges, BSA clearly violates this assumption due to surface charge heterogeneity. The result in Fig. 1, which fundamentally motivates this work, was generated in PYMOL molecular visualization software (DeLano Scientific, http://www.delanoscientific.com/) using the BSA PDB crystal structure (PDB:3V03). Although BSA solution viscosity has been widely investigated and reported as a model system, it nevertheless exhibits complex shape and charge distribution. Similar surface charge heterogeneity and more complex molecular conformations are seen in IgGs (13).

Published work on protein solution rheology spanned the range from dilute solutions to highly crowded solutions (concentrations >100 mg/mL (8–10,13–15). They invoked
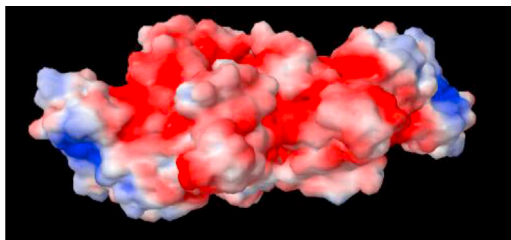

FIGURE 1 Surface charge distribution on the BSA molecule at its pI (pH 4.95), generated by the software PYMOL using the three-dimensional crystal structure of BSA from the Protein Data Bank (PDB:3V03; www.wwpdb.org). (*Red*, *white*, and *blue*) Negatively charged, positively charged, and neutral regions, respectively.

either theoretical or empirical models from colloidal dispersion rheology to explain the concentration-dependence of solution viscosity in the dilute or concentrated limit. The invocation of colloidal models to describe protein solution rheology is intuitively appealing, because proteins squarely fall within the colloidal domain on account of their charge and size (16). The seminal work of Tanford and Buzzell (15) focused on the viscosity of BSA solutions up to a concentration of ≈ 40 mg/mL between pH 4.3 and 10.5. A minimum in the relative viscosity as a function of pH was reported and explained by invoking arguments related to the primary electroviscous effect (3,15). Ross and Minton (17) developed a semiempirical model based on the Mooney equation, which was originally developed for filled elastomers. They demonstrated that corrections to the Mooney equation successfully describe the concentration-dependence of viscosity of Hemoglobin solutions up to concentrations of 400 mg/mL, if one accounts for particle shape and specific volume through the Simha factor (18) and the specific volume of the protein (17,18). However, applying models that describe the concentration dependence of viscosity of hard-sphere dispersions to protein solutions is questionable even if compressibility and shape are accounted for, because the macromolecular surface is heterogeneous and the interaction potential for proteins typically involves both Derjaguin-Landau-Verwey-Overbeek (DLVO) (19) and non-DLVO forces (i.e. hydrophobic interactions and hydration forces) (5,19–21).

Another reason to critically interrogate the applicability of colloidal dispersion rheology models to concentrated protein solutions is that these models typically assume monodispersity. However, in solution, protein monomers can exist in dynamic equilibrium with reversible clusters, and can also form nonequilibrium/irreversible clusters (5,6,22). Essential protein-specific biophysics, such as pH- and concentration-dependent conformation (1,2) and the spatial heterogeneity of charge, are left unaddressed in these models.

An incisive experiment to examine the validity of colloidal models in protein solution rheology would probe the concentration-dependent viscosity over a broad protein concentration range while varying pH to tune the competi-

tion between short-range attraction and long-range repulsion. Some published literature studies were limited to either a single pH or a much narrower pH range than the range studied here (15,24–30) (also see Table S2 in the Supporting Material). This limited experimental range, and the use of an inappropriate definition for protein volume fraction that ignores surface hydration, has led to the apparent conclusion that colloidal rheology models apply to protein solutions. We found that the model of Russel et al. (20) fitted the concentration-dependence of viscosity of BSA solutions at pH 3.0, 4.0, and 5.0 but failed at higher pH (6.0 and 7.4). The empirical hard-sphere model of Krieger and Dougherty (21) did not describe the concentration-dependence of BSA viscosity when we held the measured intrinsic viscosity constant in fits while only letting the maximum packing volume fraction float freely. We demonstrate the hitherto unappreciated critical need to account for molecular hydration in the calculation of fundamental protein hydrodynamic quantities such as intrinsic viscosity, which has been selectively accounted for in Iino and Okuda (31), leading to the apparent result that BSA is a hard sphere. We found that the hydration-corrected intrinsic viscosity of BSA did not attain its hard-sphere value (2.5) between pH 3.0 and 7.4.

MATERIALS AND METHODS

Lyophilized BSA powder ((Cat. No. A7906; Sigma-Aldrich, St. Louis, MO) >99.7% protein, essentially fatty-acid free) of molar mass = 67 KDa, was dissolved at 20 mM ionic strength (I) in buffers comprising sodium citrate/citric acid (pH 3.0), sodium acetate/acetic acid (pH 4.0 and pH 5.0 respectively), histidine hydrochloride (pH 6.0), and phosphate-buffered saline (pH 7.4) (see Acknowledgements). Under these low (20 mM) ionic strength conditions, published literature demonstrated no significant aggregation in BSA solutions. However, under moderate salt conditions, aggregation was pronounced (33). Stock solutions were prepared at 500 mg/mL by dissolving the appropriate mass of lyophilized BSA in 125 mL of 0.02 μm prefiltered buffer (Anotop 10 syringe filter, Lot No. D140746; Whatman, GE Healthcare, Piscataway, NJ) and allowing for complete quiescent dissolution between 2 and 8°C for up to 72 h, and were filtered through 0.22 μm filters of poly(ethersulfone) membranes (Thermo Scientific, Billerica, MA). They were gravimetrically diluted to the final concentration (c_{BSA}), which was measured using absorbance at λ (wavelength) = 280 nm (A_{280}) on a model No. 8453 UV-visible spectrophotometer (Agilent Technologies, Santa Clara, CA). An absorbance coefficient of ε_{280} = 0.667 mL/mg-cm (12) was used for BSA. All solutions were stored between 2 and 8°C until use.

Size exclusion chromatography (SEC) was performed on 10 mg/mL samples: 250 μg mass was injected into a UV-detector-equipped model No. 1100 series HP-SEC (Agilent Technologies) loaded with a model No. G3000WXL column (Tosoh Bioscience, South San Francisco, CA) of 25 nm average pore size. The HP-SEC mobile phase contains 100 mM anhydrous dibasic sodium phosphate (J.T. Baker Cat. No. 5062-05; Mallinckrodt Baker, Phillipsburg, NJ), 100 mM sodium sulfate (J.T. Baker Cat. No. 3898-05; Mallinckrodt Baker), and 50 μM sodium azide at pH 6.8 (titrated with hydrochloric acid). Sodium azide acts as an antimicrobial agent. SEC-multiangle light-scattering was also performed (see Fig. S1 and Table S1 in the Supporting Material) to determine the molar masses of monomer and clusters.

Dynamic light scattering was used to measure the mutual diffusion coefficient D_m of BSA solutions between c_{BSA} = 2 mg/mL and 12 mg/mL on a DynaPro plate reader (Wyatt Technology, Santa Barbara, CA) with a

detector sensitive to $\lambda = 833$ nm and at fixed scattering angle $(\theta) = 130°$. A linear fit of D_m versus c_{BSA}, $D_m = D_o(1+k_D c_{BSA})$ [34,35], was used to obtain the diffusion interaction parameter, k_D [19], which measures intermolecular thermodynamic and hydrodynamic contributions. The aforementioned equation is a generalization of the result derived by Batchelor [35], who determined $k_D = 1.45$ for hard spheres with no-slip boundary conditions for a purely hydrodynamic problem. Positive and negative k_D values signify net repulsive and attractive intermolecular interactions, respectively. Of course, D_m and η contain contributions from both thermodynamic (DLVO and non-DLVO contributions) and hydrodynamic interactions in crowded protein solutions. Static light-scattering measurements were performed on a Zetasizer Nano (Malvern Instruments, Malvern, Worcestershire, UK) with $\theta = 90°$ and $\lambda = 533$ nm to construct a Debye-Zimm plot from the average scattering intensities using the analysis [36–38]

$$Kc/R_\theta = 1/M_w + 2B_{22}c_{BSA},$$

where Kc/R_θ and B_{22} denote the excess Rayleigh ratio and second virial coefficient, respectively.

Infinite shear rate viscosity was measured over a shear rate $(\dot{\gamma})$ range of 3×10^4 s^{-1} $\leq \dot{\gamma} \leq 1.2 \times 10^5$ s^{-1} using a microfluidic viscometer/rheometer on a chip (m-VROC; Rheosense, San Ramon, CA) equipped with a Type-D chip (see details in Pathak et al. [9]).

RESULTS AND DISCUSSION

We first examined dilute solution behavior to characterize the species in solution. SEC chromatograms of BSA solutions buffered between pH 3.0 and 7.4 (Fig. 2) quantify relative populations of monomer and higher-order clusters in solution. Published work [23–28] failed to report this essential biophysical characterization and applied viscosity models while a priori assuming monodispersity and a fixed conformation, which are invariant to molecular shape and concentration. SEC measures the fraction of soluble species (monomers and larger clusters), which is indispensable for understanding and modeling the concentration-dependent solution viscosity because the measured viscosity reflects the sum-total contributions of all these species. Clearly, the BSA solutions studied here were polydisperse, which governed interpretation of the concentration-dependence of viscosity and fitting of colloidal models to protein solution rheology data. The polydispersity reported here is in qualitative accord with published data on BSA [39].
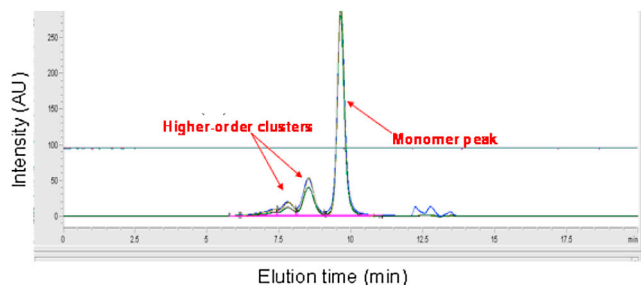

FIGURE 2   SEC chromatograms for BSA at 10 mg/mL and pH = 3.0 (*navy blue*), 4.0 (*green*), 5.0 (*blue*), and 7.4 (*orange*). (*Inset*) Same data, but magnified to emphasize elution times for higher-order clusters.

Peak integrations provide direct access to the percentage of monomer ($\approx 70\%$) and higher-order clusters ($\approx 30\%$). SEC multiangle light-scattering measurements confirm that the elution peak at ~9.5 min corresponds to BSA monomer (see Table S1). At all other pHs, the percentage of monomer is $\approx 76\%$ and higher-order clusters are $\approx 24\%$. It is worth noting that each injection was infinitely diluted in the pH 6.8 buffered HP-SEC mobile phase inside the column; therefore, the populations of monomer and higher-order species may change with pH and concentration. Our conclusions, however, were unaffected by the limitations of the SEC data, because the models we interrogate assume monodispersity that is invariant with concentration and pH.

We next examine how the pH-dependent intermolecular interactions affect the concentration-dependence of viscosity of BSA solutions. To quantify the role of attractive and repulsive interactions, we determined the concentration-dependence of D_m, obtained from the dynamic light-scattering measurements for c_{BSA} between 2 and 12 mg/mL (Fig. 3 A). The pH-dependence of D_m is reminiscent of the classical behavior of mutual diffusion coefficients in repulsive and attractive colloidal dispersions [20,34]. Electrostatic repulsions accelerate concentration fluctuations and dynamics in repulsive systems [27]. However, due to stronger protein-protein attractions at the pI, concentration fluctuations slowed down and D_m decreased as concentration increased [20,33,37]. Electrostatic repulsion clearly dominates at pH $\neq$ pI. D_m vs. c_{BSA} is notably smallest in magnitude at pH 3.0, due to conformational changes of the BSA monomer at low pH because the BSA monomer exists in a partially-unfolded state for concentrations ≤ 10 mg/mL [23]. Partially unfolded proteins experience greater hydrodynamic drag relative to the completely folded monomer, due to the increase in effective hydrodynamic diameter [3,18,23,35]. These results are qualitatively consistent with published data reported for BSA between pH 4.0 and 7.4 at a fixed ionic strength of 15 mM [27]. Slight numerical differences from reported values therein are likely due to differences in ionic strength between our two studies as well as differing BSA lot numbers. The measured k_D and B_{22} values clearly showed strong electrostatic repulsion at pH distinct from the pI. Surface charge increases the effective diameter of a protein or a colloidal particle, and affects the viscosity of the protein solution or colloidal dispersion through Stokes law considerations.

We now address how colloidal rheology models describe composition-dependence of BSA solution viscosity at varying pH, which controls net charge on protein molecules. Because colloidal rheology models couch the definition of colloid concentration in terms of volume fraction (ϕ), we must first define the protein volume fraction in solution to objectively evaluate these models. The first definition of ϕ that we invoke in Eq. 1 below is the classical polymer solution definition [36]. Because it has been applied to
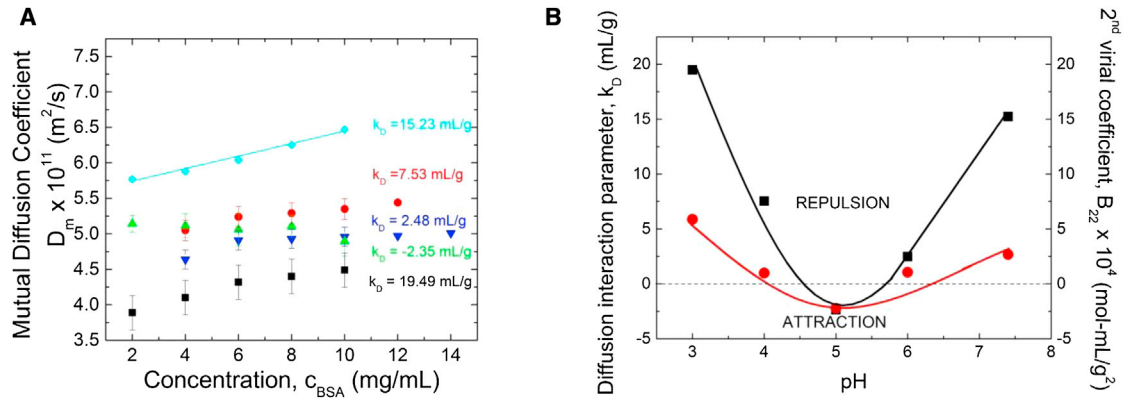
FIGURE 3   (A) BSA mutual diffusion coefficient (D_m) for BSA concentration, c_{BSA}, of 2 mg/mL $\leq c_{BSA} \leq$ 12 mg/mL at pH = 3.0 (*squares*), 4.0 (*circles*), 5.0 (*triangles*), 6.0 (*inverted triangles*), and 7.4 (*diamonds*). (B) BSA second virial coefficient, B_{22}, from static light scattering (*circles*) and the diffusion interaction parameter, k_D (*squares*) from dynamic light scattering versus pH. The uncertainties (one standard deviation; determined from the average of five measurements on fresh samples) are smaller than the symbol size.

protein solutions phenomenologically (insofar as it ignores surface hydration (25)), we refer to it as the "apparent volume fraction",

$$\varphi = \frac{cN_A V_H}{M_w}, \qquad (1)$$

where N_A and V_H denote Avogadro's constant and BSA monomer hydrodynamic volume, respectively.

Although we considered an alternate definition of ϕ also used by other groups (24,43), we went well beyond their use of this definition to scrutinize the validity of colloidal models in crowded protein solution rheology. This definition rigorously accounts for the protein hydration layer via the pH-dependent protein partial specific volume $\overline{\nu_p}$ (2,3), which includes the hydration layer by definition. Specific volume is a critical thermodynamic property (2) that quantifies solute-solvent interactions and protein hydration (40). It depends on intrinsic protein volume (van der Waals volume), changes in volume of surrounding solvent due to protein addition, and protein interactions with all other solution component molecules (2). Whereas appropriate accounting for the hydration-layer effects on protein solution hydrodynamics via $\overline{\nu_p}$ (sedimentation, translational and rotational friction/diffusion coefficient, and viscosity) is critical (2,3), it has not been performed in the context of colloidal rheology model fits to protein solution viscosity. Thus, the protein and the solvent are inseparable, because hydration water is critical for protein structure and function (31,40–43). The extent of hydration, of course, depends on the ratio of dry mass to water added. For a fully hydrated protein, $\overline{\nu_p}$ saturates to constant value over a certain weight fraction of water added (41,42),

$$\phi = \frac{m_{BSA}\overline{\nu_p} + \delta\overline{\nu_w}}{V_w + m_{BSA}\overline{\nu_p} + \delta\overline{\nu_w}}, \qquad (2)$$

where V_w and m_{BSA} denote solvent (water) volume and BSA mass, respectively, while δ and $\overline{\nu_w}$ denote the mass

of hydration (bound) water per gram of BSA (0.4 g bound water per g BSA (61,62)) and the partial specific volume of water, respectively. The definition of ϕ in Eq. 2 accounts for the dry (bare) protein and the hydration layer through the $m_{BSA}\overline{\nu_p}$ and $\delta\overline{\nu_w}$ terms, respectively. In the context of macromolecular hydrodynamics (viscosity, translational and rotational friction, and the drag aspects of sedimentation), both the bare protein and the hydration layer need to be invoked (61,62). In general, $\overline{\nu_p}$ is expected to change with pH for proteins due to protonation or deprotonation below and above the pI. El Kadi et al. (43) have determined $\overline{\nu_p}$ for BSA to vary between 0.727 and 0.742 mL g^{-1} between pH 2.0 and 8.0, respectively. In our calculations, we use pH-dependent $\overline{\nu_p}$ reported by El Kadi et al. (43), but hold δ constant (independent of pH).

We now compare these two definitions of ϕ in the context of colloidal rheology models, starting with the model of Russel et al. (20), which accounts for uniform surface charge, inherent to dilute charge-stabilized colloidal dispersions. It provides an electrostatic correction to the quadratic term in the Einstein-Batchelor equation (35), which signifies two-body hydrodynamic interactions:

$$\frac{\eta(\varphi)}{\eta_s} = 1 + 2.5\varphi + \left(2.5 + \frac{3}{40}\left(\frac{d_{\text{eff}}}{2a}\right)^5\right)\varphi^2 + O(\varphi^3)$$

$$= 1 + 2.5\varphi + s\varphi^2 + O(\varphi^3). \qquad (3)$$

In Eq. 3, $2a$ and d_{eff} (= $2a$ for hard spheres) are the actual and effective hard sphere diameters, respectively, η_s is the buffer viscosity. Because d_{eff} increases due to electrostatic repulsion at pH distinct from pI, the coefficient, s, of the quadratic term in Eq. 3, therefore, relates to hydrodynamic and thermodynamic contributions in colloidal dispersions and protein solutions.

The ϕ dependence of the relative viscosity ($\eta_r = \eta/\eta_s$) with ϕ defined using Eq. 1, of BSA solutions, is illustrated in Fig. 4 A between pH 3.0 and 7.4 along with nonlinear
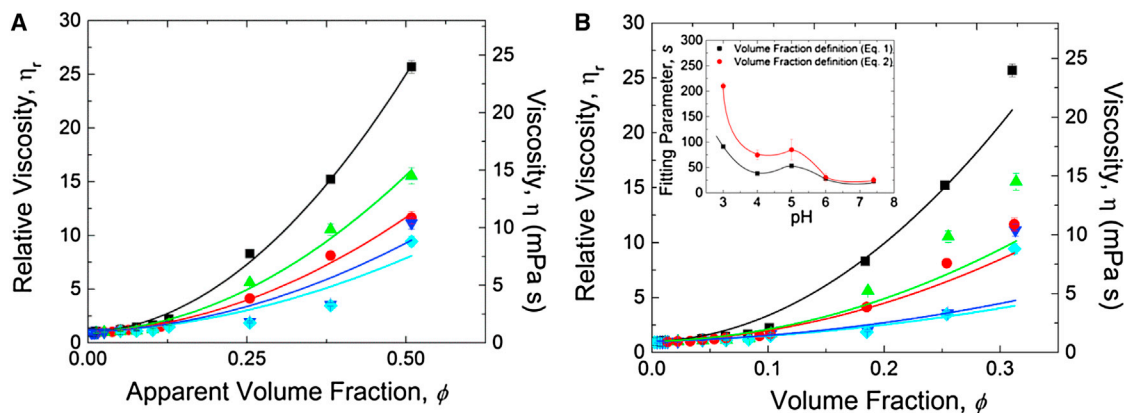
FIGURE 4 (*A*) BSA solution relative viscosity η_r versus volume fraction ϕ (defined by Eq. 1) for 2 mg/mL $\leq c_{BSA} \leq$ 400 mg/mL at pH = 3.0 (*squares*), 4.0 (*circles*), 5.0 (*triangles*), 6.0 (*inverted triangles*), and 7.4 (*diamonds*). Curves denote fits to the model of Russel et al. (20) (Eq. 3). (*B*) η_r vs. ϕ (defined by Eq. 2). Viscosity data are at shear rate $\dot{\gamma} = 10^4 \text{ s}^{-1}$ (in the infinite shear plateau). The uncertainty in viscosity (standard deviation) was determined from five different measurements with fresh sample loadings. In some cases, the uncertainties are smaller than the symbol sizes. (*Inset*) Model from Russel et al. (20), (Eq. 3) fitting parameter, s, extracted from panels *A* and *B*, with ϕ calculated using Eqs. 1 and 2 (*squares* and *circles*, respectively).

least-squares regression fits of the model of Russel et al. (20) to the data. By applying the Levenberg-Marquardt algorithm (44,45), with s being the only adjustable parameter, the model of Russel et al. (20) suggests that for proteins bearing zero net charge at the pI, $d_{eff} \approx 2a$. While the model of Russel et al. (20) described the data between pH 3.0 and 5.0, model predictions departed from experimental data at pH > 5.0, likely due to the rather sharp rise in viscosity between 300 mg/mL and 400 mg/mL. BSA undergoes conformational changes at pH 3.0, which invariably contribute to an increase in d_{eff} and η_r. Therefore, surface charge is not the only contribution to the strong ϕ-dependence of η_r for pH < 5.0. We recovered qualitatively similar results for calculating ϕ rigorously using Eq. 2; see Fig. 4 *B*. The model of Russel et al. (20) thus lacks sufficient generality to describe the full pH- and concentration-dependence of BSA solution rheology. The subtleties associated with BSA solution biophysical chemistry such as conformational changes that occur at pH 3.0, and the heterogeneous surface charge distribution, are ignored in the model of Russel et al. (20).

Because the $O(\phi^2)$ coefficient, s, in Eq. 3 reflects both hydrodynamic and thermodynamic contributions to η, we examine whether its magnitude extracted from the fits to the data in Fig. 4 *A* shows similar dependence on pH as those seen for k_D and B_{22}. If these dependences are similar, a correlation between dilute solution physicochemical parameters and s would be implied. Because Connolly et al. (46) recently suggested a similar weak correlation between k_D and η for some monoclonal antibody solutions, we examine BSA data for any similar correlations. Although Russel et al. (20) suggest that the magnitude of s should be minimal when $B_{22}/B_{22,HS} = 1$, where $B_{22,HS}$ denotes the hard sphere B_{22}, its magnitude at the extremes of pH does not correlate well with B_{22} here (*inset*, Fig. 4 *B*). Moreover, between pH 4.0 and 7.4, s attains a maximum at pH = 5.0, contrary

to the expected minimum and similar to the observed pH-dependence of η of BSA for concentrations >100 mg/mL (27) between pH 4.0 and 7.4. We therefore infer that the weak correlation between dilute and concentrated solution properties suggested by Connolly et al. (46) is invalid for BSA solutions.

We next evaluated whether the Krieger-Dougherty model (21) can describe the concentration-dependence of viscosity of concentrated BSA solutions. This model has been applied to hard sphere dispersions (20,21) and also to protein solutions with equilibrium clustering (47). It is also applied to systems with arbitrary nonspherical particle shapes and molecular conformations (21),

$$\eta_r = \frac{\eta}{\eta_s} = \left(1 - \frac{\varphi}{\varphi_m}\right)^{-[\eta]\varphi_m}, \qquad (4)$$

where ϕ_m and $[\eta]$ denote maximum packing fraction and intrinsic viscosity, respectively. Whereas Eq. 4 has been applied to crowded protein solution rheology (25) by defining ϕ via Eq. 1, its validity must be critically interrogated while accounting for protein hydration (Eq. 2). To minimize the number of freely floating parameters, we determine and fix $[\eta]$ from dilute solution viscosity data (2 mg/mL $\leq c_{BSA} \leq$ 12 mg/mL) using the method from the literature (48,49). The value of $[\eta]$ is determined from the slope of a plot of $1-1/\eta_r$ vs. ϕ (see Fig. S2 and Fig. S3). Table 1 summarizes pH-dependence of $[\eta]$. Clearly $[\eta]$ is largest at pH 3.0, in agreement with prior studies (29).

BSA exists in a partially-unfolded state at pH 3.0 for concentrations nominally $\leq$10 mg/mL (23). Between pH 4.0 and 8.0, however, we find that $[\eta]$ varies significantly, in contrast with reports in Tanford and Buzzell (15), where it is implied that dilute BSA solutions exhibit no significant conformational transitions between pH 4.3 and 10.5. This

TABLE 1   Intrinsic viscosity, [η], obtained using polymer definition of volume fraction (Eq. 1) and with hydration correction for volume fraction (Eq. 2)

pH	Experimental intrinsic viscosity, [η] from fit to Eq. 4 using ϕ defined in Eq. 1	Experimental intrinsic viscosity, [η] from fit to Eq. 4, using ϕ defined in Eq. 2
3.0	7.91 ± 0.51	9.06 ± 0.57
4.0	4.19 ± 0.69	4.81 ± 0.79
5.0	5.33 ± 0.61	6.10 ± 0.69
6.0	3.21 ± 0.12	3.72 ± 0.14
7.4	2.86 ± 0.28	3.27 ± 0.33

observation suggests that the shape, conformation, and polydispersity of BSA molecules and their aggregates, as embodied in [η], changes between dilute and crowded solutions and with pH. BSA apparently approaches the hard-sphere limit, [η] = 2.5, at pH 6.0 and 7.4, only if one naïvely defines ϕ by Eq. 1. When hydration is invoked (Eq. 2), the hard sphere intrinsic viscosity (2.5) is never established for BSA at the solution conditions studied here. Overemphasis on colloidal properties of proteins at the expense of their macromolecular identity has led to the incorrect conclusion that BSA is a hard sphere. The value of δ (see Eq. 2) chosen here (i.e. 0.4) is at the upper end of the range reported in the literature. We chose this value to demonstrate that [η] never reaches 2.5 (the hard sphere value). When smaller values of δ are chosen instead, the resulting values of [η] become even larger.

We can now interrogate fits of the Krieger-Dougherty model (21) to our data using nonlinear least-squares regression, with ϕ_m kept as the only floating parameter, because [η] is easily experimentally determined. Clearly, as seen in Fig. 5 A, predictions of the Krieger-Dougherty model (21) disagree with data for relatively low ϕ (≈ 0.1) between pH 3.0 and 6.0. Similar behavior has been reported in the literature for BSA at high concentrations, where clear deviations from hard sphere models were observed (22). The ϕ-values calculated from Eq. 2 are much smaller than those

from Eq. 1. The absence of the hydration correction in Eq. 2 and narrow pH-range investigations of BSA solution viscosity have possibly led others to the erroneous conclusion that colloidal viscosity models work well at high BSA concentrations (26–28). The hydration correction, Eq. 2, also strongly affects the curvature of $\eta(\phi)$. Finally, when we defined ϕ in Eq. 2 and let ϕ_m and [η] both float freely, as had also been done by Sharma et al. (25), we recover their result that the model of Krieger and Dougherty (21) apparently fits the viscosity of BSA solutions until an upper-concentration limit of 250 mg/mL at pH 7.4 (see Fig. S4). This validation step generated confidence in the robustness of our nonlinear regression algorithm.

The Krieger-Dougherty model (21) can account for particle shape (a determinant of protein solution viscosity/diffusivity/sedimentation coefficient, along with hydration) through [η], which is a dilute solution parameter by definition. However, its major limitation is that it does not appropriately account for the effect of particle compressibility. Variations in compressibility reflect conformational changes (43) that are particularly important in the case of proteins and microgels: particle deformation in microgels and molecular conformation in proteins at high concentrations might significantly affect their rheology (43,50). The ϕ_m of protein solutions and microgels can far exceed the random-close packing limit for hard spheres, which is $\approx \phi \approx 0.64$ for monodisperse hard spheres and $\phi = 0.71$ for prolate ellipsoids (51). Because the Krieger-Dougherty model (21) fits the data too poorly, we cannot assign physical meaning to ϕ_m, even if hydration is accounted for (Fig. 5 B).

CONCLUSIONS

In summary, we have demonstrated the breakdown of the colloidal description of buffered BSA solution viscosity across broad pH and concentration ranges. The model of Russel et al. (20), while successful in capturing composition-dependence of viscosity at pH 3.0, 4.0, and 5.0, failed
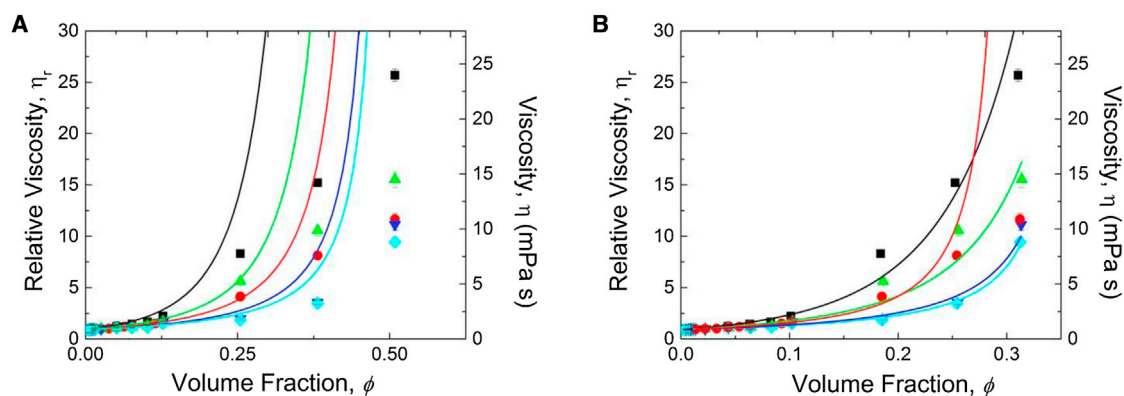

FIGURE 5   (A) BSA relative viscosity η_R versus volume fraction ϕ (same data and symbol keys as Fig. 4). Curves are fits to the Krieger-Dougherty model (21) (Eq. 4) with ϕ defined by Eq. 1. (B) Same experimental data as in Fig. 5 A and Fig. 4; curves are fits to the Krieger-Dougherty model (21) (Eq. 4) with ϕ defined by Eq. 2. Infinite shear plateau viscosity values correspond to a shear rate of $\dot{\gamma} = 10^4$ s^{-1}.

to model the data at pH 6.0 and 7.4. The Krieger-Dougherty model (21) failed at high BSA concentrations exceeding 100 mg/mL for pH 3.0, 4.0, and 5.0, though it succeeded at pH 6.0 and 7.4. Our rigorous analysis and careful conclusions radically differ from all prior studies that proclaimed the success of colloidal dispersion models for understanding protein solution rheology (17,25,28,31). We ascribe their incorrect conclusion to their experimental designs being limited to a single ionic strength or pH, or to narrow ranges of both. The pH-dependent chain conformation and spatially heterogeneous charge distribution (13) influence the concentration dependent solution viscosity, and have been consistently ignored in the literature. We have demonstrated that protein solution hydrodynamics cannot be quantitatively understood without invoking surface hydration. Significantly, we found that BSA never becomes a hydrodynamic hard sphere between pH 3.0 and 7.4 across a concentration range spanning 2 mg/mL to 500 mg/mL.

Because there is extraordinarily complex physics and biophysics underlying protein solution rheology, we now propose a starting point for holistic models of protein solution rheology by unifying concepts rooted in statistical mechanics (60) and protein biophysics (3). The macroscopic viscosity represents the force per unit velocity, embodied in the friction coefficient, ζ, experienced by a protein monomer. A phenomenological expression for the shear rate-dependent viscosity can be written as

$$\eta = \eta\left\{\frac{\zeta}{\zeta_e}, \frac{\zeta_e}{\zeta_o}, M_w, \varphi_{\text{monomer}}, \varphi_{\text{cluster}}, Z(pH), I, [\eta], u(r), \dot{\gamma}\right\}.$$
(5)

The value of η depends on molar weight (M_w) and monomer volume fraction (ϕ_{monomer}). Friction contains contributions from shape/shape asymmetry (ζ_e/ζ_o) and hydration factor (ζ/ζ_e) (52,53). Here ζ_o denotes the Stokesian friction coefficient of an anhydrous spherical particle with the same mass and partial specific volume as the protein being considered. Clearly, the importance of protein hydration and conformation/shape for understanding solution physical chemistry and transport properties are mainstream ideas in protein biophysics that need to be bridged to solution rheology models. Of course, when clusters coexist with monomers in solution (9,56), cluster volume fraction (ϕ_{cluster}) is also reflected in viscosity. Clusters can precipitate from solution too (9), significantly complicating any theoretical description of unstable protein solution hydrodynamics, because the system becomes both a solution and a suspension. However, that problem is significantly more complicated than the current case of BSA solutions. Protein conformation (49) is also reflected in solution hydrodynamics and rheology. In dilute protein solutions, [η] contains conformational information (52–55); but in concentrated solutions with nonnegligible intermolecular interactions, the small-angle scattering intensity, $I(q)$, at large wavevectors (q) (23,26,57–59) contains chain conformation information. The intermolecular potential $u(r)$ can be extracted from $I(q)$, the structure factor $S(q)$, and the form factor, $P(q)$. Current models liberally approximate these constitutive inputs to protein solution viscosity.

Appropriate biophysical and statistical mechanical models that account for monomers, clusters, hydration, charge (distribution), and intermolecular forces to solution viscosity are currently being developed by our team for globular proteins and immunoglobulins by leveraging our recent SANS (Small-Angle Neutron Scattering) data over a wide range of pH and concentration. Our future contributions will elucidate the transitions in concentrated BSA solution conformation between pH 3.0 and 7.4.

SUPPORTING MATERIAL

SEC-MALLS analytical principle and data (Fig. S1 & Table S1), SEC data (Table S2), intrinsic viscosity determination plots (Figs. S2 & S3), DLS data (Fig. S5) and supporting references (including a list of prior reports on BSA solution rheology, Table S3) are available in the Supporting Material. The sensitivity of fitting the Krieger-Dougherty model (Eq. 5) to experimental viscosity data by letting both intrinsic viscosity and maximum packing volume fraction float freely as fit parameters is also shown in Fig. S4 as well as References (63–72) are available at http://www.biophysj.org/biophysj/supplemental/S0006-3495(13)01142-9.

REFERENCES

1. Zhou, H. X., G. Rivas, and A. P. Minton. 2008. Macromolecular crowding and confinement: biochemical, biophysical, and potential physiological consequences. *Annu. Rev. Biophys.* 37:375–397.

2. Creighton, T. E. 1992. Proteins: Structures and Molecular Properties. W.H. Freeman, New York.

3. Tanford, C. 1961. Physical Chemistry of Macromolecules. Wiley, New York.

4. Homouz, D., L. Stagg, …, M. S. Cheung. 2009. Macromolecular crowding modulates folding mechanism of α/β protein apoflavodoxin. *Biophys. J.* 96:671–680.

5. Shire, S. J., Z. Shahrokh, and J. Liu. 2004. Challenges in the development of high protein concentration formulations. *J. Pharm. Sci.* 93:1390–1402.

6. Roberts, C. J., and W. Wang. 2010. Aggregation of Therapeutic Proteins. John Wiley & Sons, New York.

7. Thomas, C. R., and D. Geer. 2011. Effects of shear on proteins in solution. *Biotechnol. Lett.* 33:443–456.

8. Bee, J. S., J. L. Stevenson, …, T. W. Randolph. 2009. Response of a concentrated monoclonal antibody formulation to high shear. *Biotechnol. Bioeng.* 103:936–943.

9. Pathak, J. A., R. R. Sologuren, and R. Narwal. 2013. Do clustering monoclonal antibody solutions really have a concentration dependence of viscosity? *Biophys. J.* 104:913–923.

10. Salinas, B. A., H. A. Sathish, …, T. W. Randolph. 2010. Understanding and modulating opalescence and viscosity in a monoclonal antibody formulation. *J. Pharm. Sci.* 99:82–93.

11. Nezlin, R. 2010. Interactions between immunoglobulin G molecules. *Immunol. Lett.* 132:1–5.

12. Peters, T. 1995. All About Albumin: Biochemistry, Genetics, and Medical Applications. Elsevier, New York.

13. Yadav, S. T. M., T. M. Laue, …, S. J. Shire. 2012. The influence of charge distribution on self-association and viscosity behavior of monoclonal antibody solutions. *Mol. Pharm.* 9:791–802.

14. Kumar, V. N., N. Dixit, …, W. Fraunhofer. 2011. Impact of short range hydrophobic interactions and long range electrostatic forces on the aggregation kinetics of a monoclonal antibody and a dual-variable domain immunoglobulin at low and high concentrations. *Int. J. Pharm.* 421:82–93.

15. Tanford, C., and J. G. Buzzell. 1956. The viscosity of aqueous solutions of bovine serum albumin between pH 4.3 and 10.5. *J. Phys. Chem.* 60:225–231.

16. De Young, L. R., A. L. Fink, and K. A. Dill. 1993. Aggregation of globular proteins. *Acc. Chem. Res.* 26:614–620.

17. Ross, P. D., and A. P. Minton. 1977. Hard quasispherical model for the viscosity of hemoglobin solutions. *Biochem. Biophys. Res. Commun.* 76:971–976.

18. Mehl, J. W., J. L. Oncley, and R. Simha. 1940. Viscosity and the shape of protein molecules. *Science.* 92:132–133.

19. Verwey, E. J. W., and J. T. G. Overbeek. 1999. Theory of the Stability of Lyophobic Colloids. Dover, Amsterdam.

20. Russel, W. B., D. A. Saville, and W. R. Schowalter. 1989. Colloidal Dispersions. Cambridge University Press, New York.

21. Krieger, I., and T. J. Dougherty. 1959. Mechanism for non-Newtonian flow in suspensions of rigid spheres. *Trans. Soc. Rheol.* 3:137–152.

22. Brownsey, G. J., T. R. Noel, …, S. G. Ring. 2003. The glass transition behavior of the globular protein bovine serum albumin. *Biophys. J.* 85:3943–3950.

23. Barbosa, L. R., M. G. Ortore, …, R. Itri. 2010. The importance of protein-protein interactions on the pH-induced conformational changes of bovine serum albumin: a small-angle x-ray scattering study. *Biophys. J.* 98:147–157.

24. Heinen, M., F. Zanini, …, G. Nägele. 2012. Viscosity and diffusion: crowding and salt effects in protein solutions. *Soft Matter.* 8:1404–1419.

25. Sharma, V., A. Jaishankar, …, G. H. McKinley. 2011. Rheology of globular proteins: apparent yield stress and interfacial viscoelasticity of bovine serum albumin solutions. *Soft Matter.* 7:5150–5160.

26. Gaigalas, A. K., V. Reipa, …, J. Edwards. 1995. A non-perturbative relation between the mutual diffusion coefficient, suspension viscosity, and osmotic compressibility: application to concentrated protein solutions. *Chem. Eng. Sci.* 50:1107–1114.

27. Yadav, S., S. J. Shire, and D. S. Kalonia. 2011. Viscosity analysis of high concentration bovine serum albumin aqueous solutions. *Pharm. Res.* 28:1973–1983.

28. Tanford, C., J. G. Buzzell, …, S. A. Swanson. 1955. The reversible expansion of bovine serum albumin in acid solutions. *J. Phys. Chem.* 77:6421–6427.

29. Reference deleted in proof.

30. Jachimska, B., M. Wasilewska, and Z. Adamczyk. 2008. Characterization of globular protein solutions by dynamic light scattering, electrophoretic mobility, and viscosity measurements. *Langmuir.* 24:6866–6872.

31. Iino, M., and Y. Okuda. 1997. Concentration dependence of Brownian motion and the viscosity of hemoglobin solutions. *Jpn. J. Appl. Phys.* 36:3786–3790.

32. Reference deleted in proof.

33. Kronman, M. J., M. D. Stern, and S. N. Timasheff. 1956. On the aggregation of bovine serum albumin in acid pH. *J. Phys. Chem.* 60:629–633.

34. Petsev, D. N., and N. D. Denkov. 1992. Diffusion of charged colloidal particles at low volume fractions. *J. Coll. Int. Sci.* 149:329–344.

35. Batchelor, G. K. 1976. Brownian diffusion of particles with hydrodynamic interaction. *J. Fluid Mech.* 74:1–29.

36. Rubinstein, M., and R. H. Colby. 2003. Polymer Physics. Oxford University Press, New York.

37. Pusey, P. N. 1978. Intensity fluctuation spectroscopy of charged Brownian particles: the coherent scattering function. *J. Phys. A.* 11:119–135.

38. Brown, W. 1993. Dynamic Light Scattering and Some Applications. Oxford University Press, New York.

39. Chatterjee, A., and S. N. Chatterjee. 1965. Electron microscopic studies on the serum albumin molecules. *J. Mol. Biol.* 11:432–437.

40. Murphy, L. R., N. Matubayasi, …, R. M. Levy. 1998. Protein hydration and unfolding—insights from experimental partial specific volumes and unfolded protein models. *Fold. Des.* 3:105–118.

41. Perkins, S. J. 1986. Protein volumes and hydration effects. The calculations of partial specific volumes, neutron scattering matchpoints and 280-nm absorption coefficients for proteins and glycoproteins from amino acid sequences. *Eur. J. Biochem.* 157:169–180.

42. Jaenicke, R., and M. A. Lauffer. 1969. Determination of hydration and partial specific volume of proteins with the spring balance. *Biochemistry.* 8:3077–3082.

43. El Kadi, N., N. Taulier, …, M. Waks. 2006. Unfolding and refolding of bovine serum albumin at acid pH: ultrasound and structural studies. *Biophys. J.* 91:3397–3404.

44. Levenberg, K. 1944. A method for the solution of certain problems in least squares. *Quar. Appl. Math.* 2:164–168.

45. Marquardt, D. 1963. An algorithm for least squares estimation of non-linear parameters. *SIAM J. Appl. Math.* 11:431–441.

46. Connolly, B. D., C. Petry, …, Y. R. Gokarn. 2012. Weak interactions govern the viscosity of concentrated antibody solutions: high-through-put analysis using the diffusion interaction parameter. *Biophys. J.* 103:69–78.

47. Johnston, K. P., J. A. Maynard, …, K. J. Kaczorowski. 2012. Concentrated dispersions of equilibrium protein nanoclusters that reversibly dissociate into active monomers. *ACS Nano.* 6:1357–1369.

48. McMillan, D. E. 1974. A comparison of five methods for obtaining the intrinsic viscosity of bovine serum albumin. *Biopolymers.* 13:1367–1376.

49. Harding, S. E. 1997. The intrinsic viscosity of biological macromolecules. Progress in measurement, interpretation and application to structure in dilute solution. *Prog. Biophys. Mol. Biol.* 68:207–262.

50. Mattsson, J., H. M. Wyss, A. Fernandez-Nieves, K. Miyazaki, Z. Hu, D. R. Reichman, and D. A. Weitz. 2009. Soft Colloids make Strong Glasses. *Nature.* 462:83–86.

51. Donev, A., I. Cisse, …, P. M. Chaikin. 2004. Improving the density of jammed disordered packings using ellipsoids. *Science.* 303:990–993.

52. Squire, P. G., and M. E. Himmel. 1979. Hydrodynamics and protein hydration. *Arch. Biochem. Biophys.* 196:165–177.

53. Cohn, E. J., and J. T. Edsall. 1943. Proteins, Amino Acids and Peptides. Reinhold, New York.

54. Timasheff, S. N., and M. J. Gorbunoff. 1967. Conformation of proteins. *Annu. Rev. Biochem.* 36:13–54.

55. Yang, J. T. 1961. The viscosity of macromolecules in relation to molecular conformation. *Adv. Protein Chem.* 16:323–400.

56. Cardinaux, F., E. Zaccarelli, …, P. Schurtenberger. 2011. Cluster-driven dynamical arrest in concentrated lysozyme solutions. *J. Phys. Chem. B.* 115:7227–7237.

57. Stradner, A., H. Sedgwick, …, P. Schurtenberger. 2004. Equilibrium cluster formation in concentrated protein solutions and colloids. *Nature.* 432:492–495.

58. de Schepper, I. M., H. E. Smorenburg, and E. G. D. Cohen. 1993. Viscoelasticity in dense hard sphere colloids. *Phys. Rev. Lett.* 70: 2178–2181.

59. Verber, R., I. M. de Schepper, and E. G. D. Cohen. 1997. Viscosity of colloidal suspensions. *Phys. Rev. E Stat. Phys. Plasmas Fluids Relat. Interdiscip. Topics.* 55:3143–3158.

60. Dill, K. A., and S. Bromberg. 2011. Molecular Driving Forces: Statistical Thermodynamics in Biology, Chemistry, Physics and Nanoscience. Garland Science, New York.

61. Halle, B. 2004. Protein hydration dynamics in solution: a critical survey. *Philos. Trans. R. Soc. Lond. B Biol. Sci.* 359:1207–1223.

62. Curvale, R., M. Masuelli, and A. P. Padilla. 2008. Intrinsic viscosity of bovine serum albumin conformers. *Int. J. Biol. Macromol.* 42:133–137.

63. Saluja, A., and D. S. Kalonia. 2005. Application of ultrasonic shear rheometer to characterize rheological properties of high protein concentration solutions at microliter volume. *J. Pharm. Sci.* 94:1161–1168.

64. Monkos, K. 1996. Viscosity of bovine serum albumin aqueous solutions as a function of temperature and concentration. *Int. J. Biol. Macromol.* 18:61–68.

65. Sun, S. F. 1969. The pH dependence of the reduced viscosity of modified serum albumins. *Arch. Biochem. Biophys.* 129:411–415.

66. Lee, J., and A. Tripathi. 2005. Intrinsic viscosity of polymers and biopolymers measured by microchip. *Anal. Chem.* 77:7137–7147.

67. Giordano, R., G. Maisano, …, F. Wanderlingh. 1981. Structural properties of macromolecular solutions. *J. Chem. Phys.* 75:4770–4775.

68. Oates, K. M. N., W. E. Krause, …, R. H. Colby. 2006. Rheopexy of synovial fluid and protein aggregation. *J. R. Soc. Interface.* 3:167–174.

69. Bloomfield, V. 1966. The structure of bovine serum albumin at low pH. *Biochemistry.* 5:684–689.

70. Bowen, W. R., and P. M. Williams. 2001. Prediction of the rate of cross-flow ultrafiltration of colloids with concentration-dependent diffusion coefficient and viscosity—theory and experiment. *Chem. Eng. Sci.* 56:3083–3099.

71. Chikazumi, N., and T. Ohta. 1991. Estimation of hydrodynamic volume of proteins using high-performance size-exclusion chromatography and intrinsic viscosity measurement: an attempt at universal calibration. *J. Liq. Chromatogr.* 14:403–425.

72. Ikeda, S., and K. Nishinari. 2001. On solid-like rheological behaviors of globular protein solutions. *Food Hydrocoll.* 15:401–406.

The limitations of an exclusively colloidal view of
protein solution hydrodynamics and rheology

Prasad S. Sarangapani [†], Steven D. Hudson[§],

Kalman B. Migler[§], and Jai A. Pathak [†*]

[†]Formulation Sciences Department: Drug Product Manufacturing Group, MedImmune,
One MedImmune Way,
Gaithersburg, MD 20878 USA

[§]Materials Science and Engineering Division,
National Institute of Standards and Technology,
100 Bureau Drive,
Gaithersburg, MD 20899-8544 USA

Methods

Size-exclusion chromatography multi-angle light scattering (SEC-MALS): SEC-MALS was performed using a TSK gel G3000 SW 7.8 mm×30 cm, 5µm (TOSOH Bioscience) column connected to an Agilent 1100 series equipped with a Diode Array Detector (DAD, Agilent 1100 series) and a refractive index detector (RID, Agilent 1100 series). Agilent HPLC system is connected to a Multi Angle Light Scattering (MALS) detector (DAWN EOS, Wyatt Technology, Santa Barbara, CA) equipped with a laser source 690 nm and 18 detectors at angles between 22.5 ^{o} and 147 ^{o}. All detectors were normalized based on a 90 ^{o} angle using a 2 mg/mL BSA standard (Pierce standard) and calibrated with Toluene. DAD, RID and MALS signals were imported and processed in the ASTRA V software (Wyatt Technology, Santa Barbara, CA). Mass average molar masses of all species were determined using the Zimm equation:

$$Kc/R_\theta = 1/M_w \ (1 + q^2 R_g^2 / 3) + 2B_{22}c + \dots$$

$$K = 4\pi^2 n_0^2 \ (dn/dc)^2 / N_A \lambda^4$$

n_o: refractive index,
dn/dc: refractive index increment (0.185 mL/g),
c: BSA concentration ($B_{22}c$ term is negligible as the samples are dilute),
B_{22}: second virial coefficient,
N_A: Avogadro's number,
λ: wavelength of the incident light,
R_g: radius of gyration,
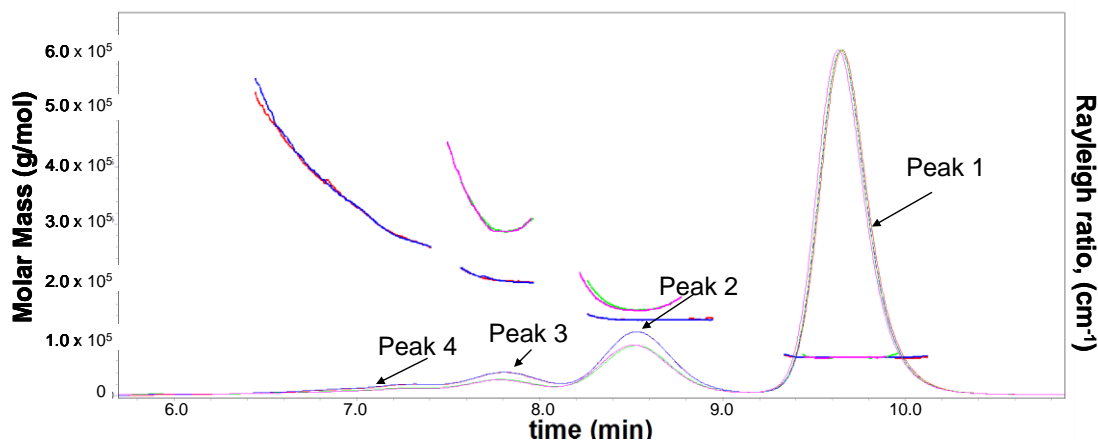q: scattering wave-vector.

Figures and Tables

FIGURE S1: Size-exclusion chromatography multi-angle light scattering (SEC MALS) measurements for BSA at 10 mg/mL and pH = 4.0 (red), 5.0 (blue), 6.0 (light blue) and 7.4 (orange). The elution peak at 9.5 minutes from the SEC chromatograms in Fig. 1 in the text as the corresponding molar mass M_w = 67 kDa approximately equals BSA monomer M_w [1]. Molar masses corresponding to peaks 1 through 4 are shown in Table S1 below.

Table S1: Molar Masses of BSA fractions obtained from SEC MALS

pH	Peak 1 (kDa)	Peak 2 (kDa)	Peak 3 (kDa)	Peak 4 (kDa)
4.0	67	134	204	328 (528-250)
5.0	67	133	204	331 (510-250)
6.0	67	162	305 (380-280)	-
7.4	67	157	316 (420-300)	-

TABLE S1: Molar masses corresponding to eluted peaks 1 through 4 in Fig. S1.

Table S2: Size-exclusion chromatography data for Bovine Serum Albumin

pH	Monomer (%)	Clusters (%)
3.0	70	30
4.0	76	24
5.0	70	30
6.0	75	25
7.4	75	25

TABLE S2: SEC data summary for Fig. 2 in the text: percentage of monomer and higher-order soluble clusters in a 10 mg/mL BSA solution from single injections (250 μg)

Table S3: Prior studies of Bovine Serum Albumin solution rheology

Authors	Concentration/Volume Fraction Range	pH range
Present work	2 mg/mL - 400 mg/mL	3.0-7.4
Sharma A. Jaishankar, Y.C. Wang, G.H. McKinley (2)	10 mg/mL - 250 mg/mL	7.4
Brownsey, G.J., T.R. Noel, R. Parker, S.G. Ring (3)	200 mg/mL - 500 mg/mL	5.4
Tanford, C. and J. G. Buzzell. (4)	40 mg/mL	4.3-10.5
Tanford, C, J.G. Buzzell, D.G. Rands, and S.A. Swanson (5)	1-15 mg/mL	2.0-10.5
Saluja, A. and D.S. Kalonia (6)	10 mg/mL - 200 mg/mL	2.0-9.0
Gaigalas, A.K., V. Reipa, J.B. Hubbard, J. Edwards, and J. Douglas (7)	Volume Fraction: 0-0.2	4.0-6.0
Monkos, K. (8)	17.6 mg/mL - 363.4 mg/mL	5.2
Sun, S.F. (9)	~1 mg/mL	2.0-11.7
Lee, J. and Tripathi, A. (10)	20 mg/mL - 80 mg/mL	8.0
Heinen, M., F. Zanini, F. Roosen-Runge, D. Fedunova, and F. Zhang (11)	Up to 500 mg/mL	7.0 (unbuffered)

Giordano, R., G. Maisano, F. Mallamace, N. Micali, and F. Wanderlingh (12)	0.1-1 mg/mL	5.2-11.8
Jachimska, B., M. Wasilewska, and Z. Adamczyk. (13)	Volume Fraction: 0.001-0.008	3.0-9.5
Curvale, R. (14)	1.25-20 mg/mL	2.4-10.0
Yadav, S., S.J. Shire, and D.S. Kalonia (15)	25-300 mg/mL	4-7
Oates, K.M.N., W.E. Krause, R.L. Jones, and R.H. Colby (16)	11-44 mg/mL	5-7.4
Bloomfield, V. (17)	1.6 mg/mL	3.6
Bowen, W.R. and P.M. Williams (18)	0-20 mg/mL	6.0, 8.0, 10.0
Chikazumi, N. and Ohta, T. (19)	1 mg/mL	2.0
Ikeda, S. and Nishinari, K. (20)	10 mg/mL	7.0

TABLE S3: Comparison of experimental design space of this work and previous BSA solution rheology investigations. The volume fraction range is shown instead of protein concentration for some references, as the authors did not define protein volume fraction (7, 13), except for ref. (11).
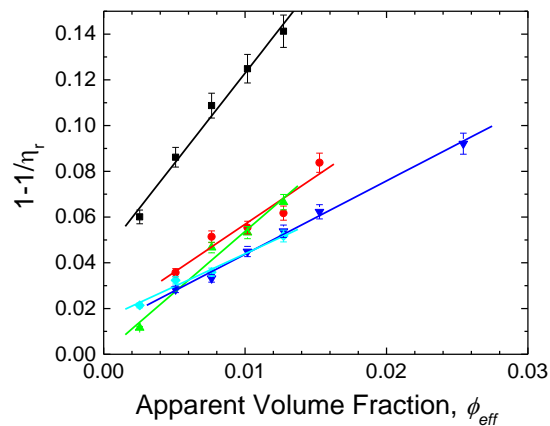
FIGURE S2: Intrinsic viscosity determination for BSA solutions at pH = 3.0 (squares), 4.0 (circles), 5.0 (triangles), 6.0 (inverted triangles), and 7.4 (diamonds) using volume fraction defined in Eq. 3 in text. The uncertainty in viscosity (one standard deviation) was determined from five different measurements with fresh sample loadings. In some cases, the uncertainties are smaller than the symbol sizes.
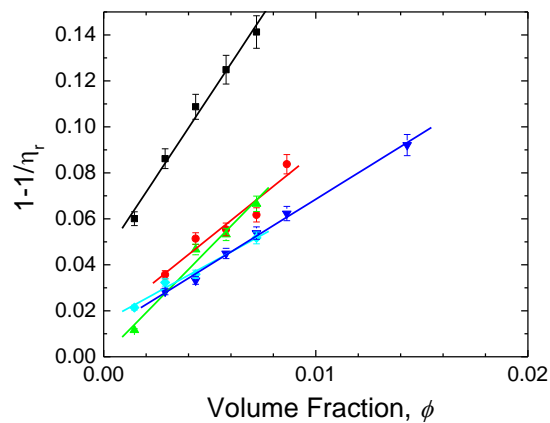

FIGURE S3: Intrinsic viscosity determination for BSA solutions at pH = 3.0 (squares), 4.0 (circles), 5.0 (triangles), 6.0 (inverted triangles), and 7.4 (diamonds) using volume fraction defined in Eq. (4) in text, which accounts for protein surface hydration. The same uncertainty in viscosity (standard deviation) applies here as in Fig. S2. In some cases, the uncertainties are smaller than the symbol sizes.
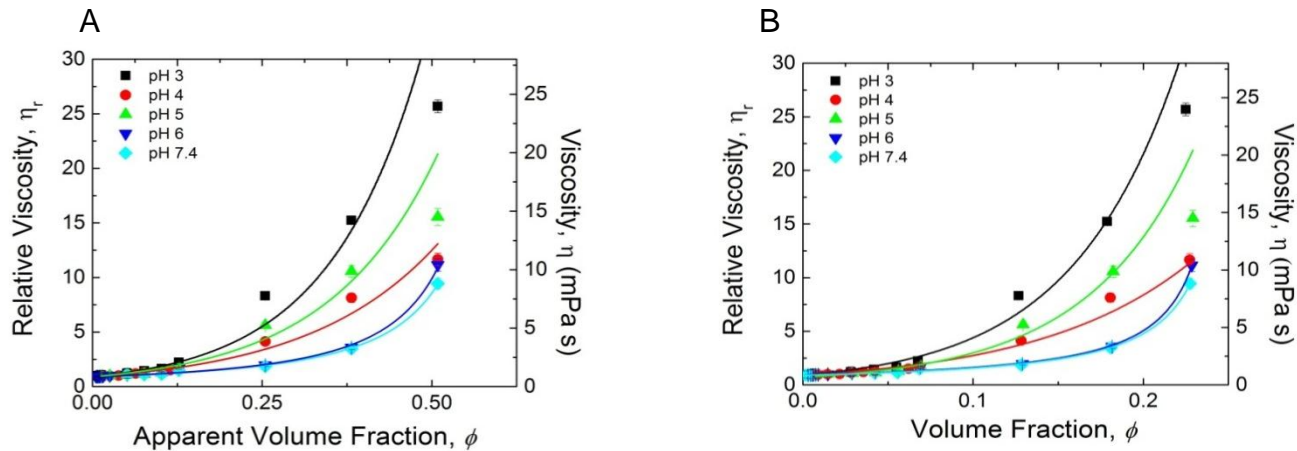
FIGURE S4: (A) Relative viscosity η_R vs. volume fraction, ϕ (calculated using Eq. 3) for BSA concentration, c_{BSA}, 2 mg/mL $\leq c_{BSA} \leq$ 12 mg/mL at pH = 3.0 (squares), 4.0 (circles), 5.0 (triangles), 6.0 (inverted triangles) and 7.4 (diamonds). (B) Same data and symbol keys as in Fig. S4(A). Curves are non-linear regression fits to the Krieger-Dougherty model (Eq. 5) with *all* parameters freely floating with ϕ defined by Eq. 3 in (A) and Eq. 4 in (B), respectively.

Size Distribution by Intensity
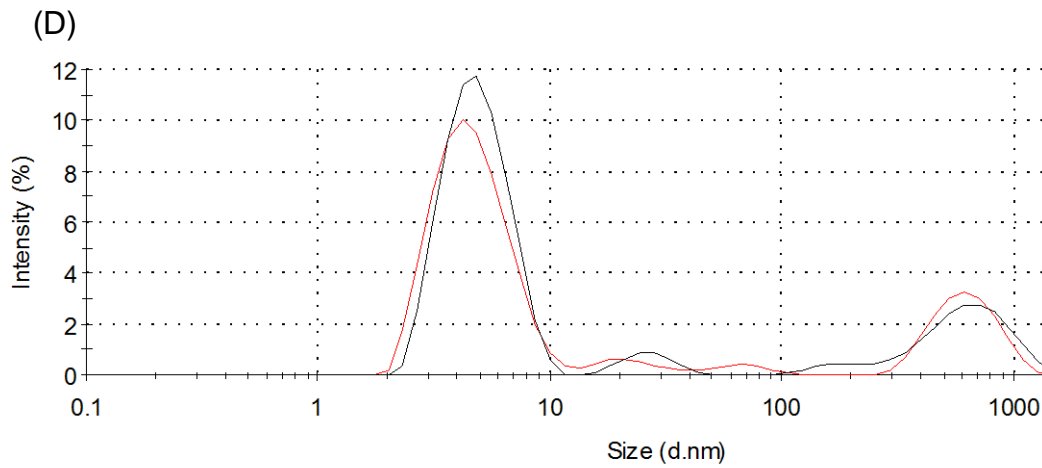
(A)

(B)

(C)

(D)
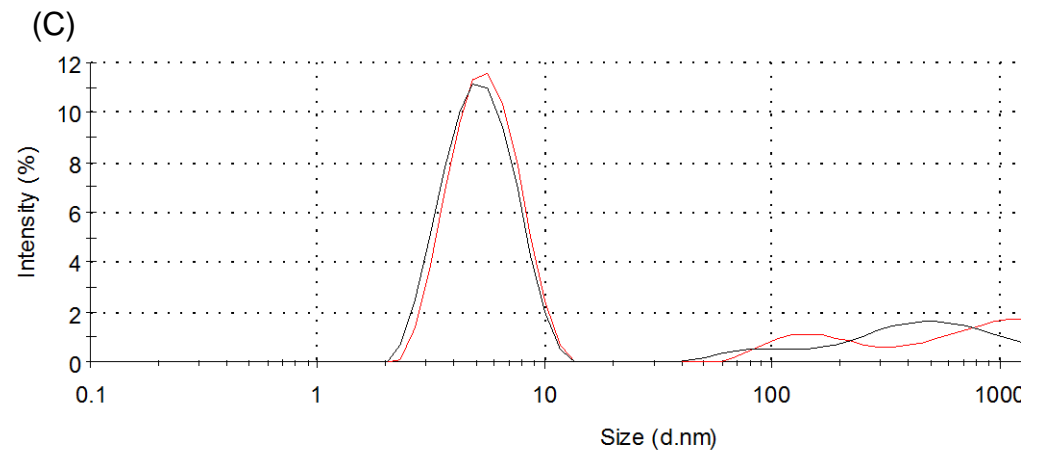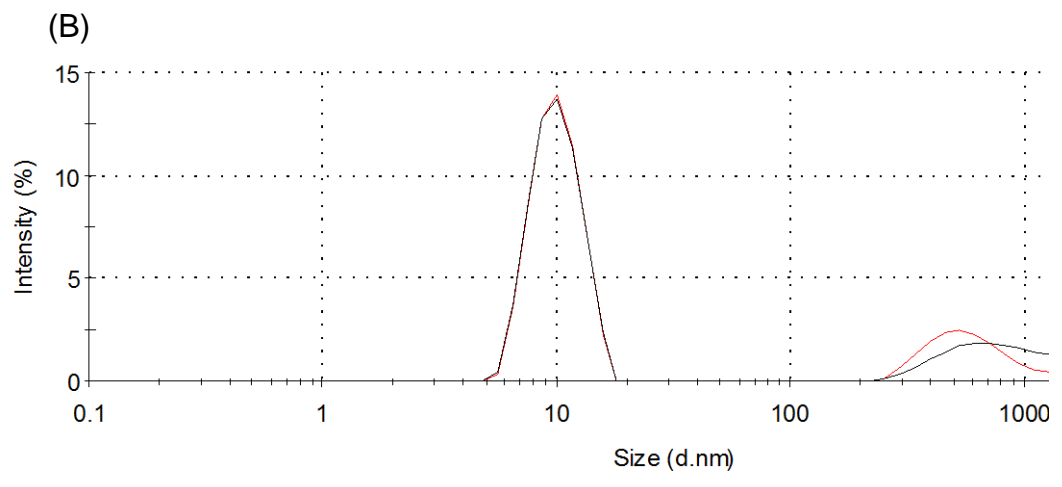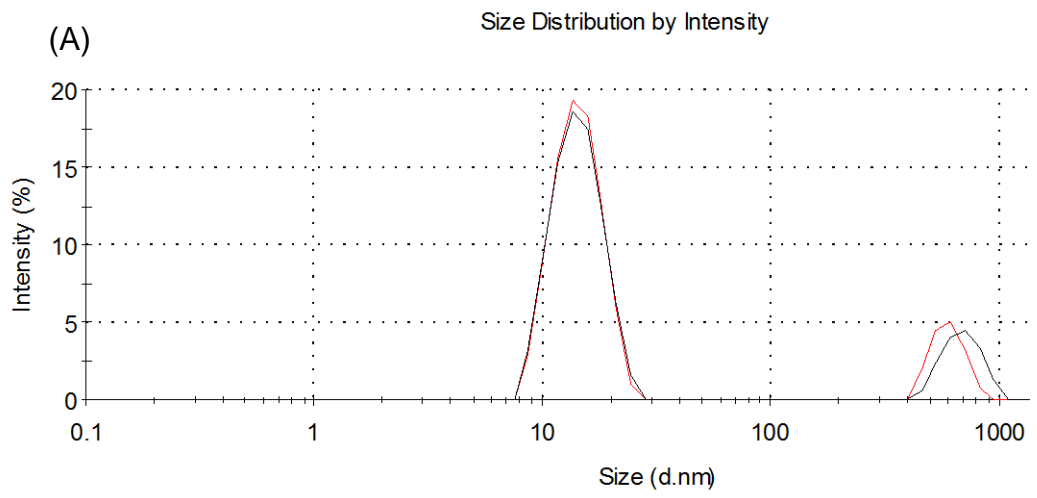
FIGURE S5: (A) Dynamic Light Scattering (DLS) data measured on a Zetasizer Nano for freshly reconstituted BSA solutions at two different time points (day 1: black, day 2: red) at 500 mg/mL and (A) pH 3, (B) pH 4, (C) pH 5, and (D) pH 7.4. Data are unreliable beyond 1 μm.

Supporting References

1. Peters, T. 1995. All About Albumin: Biochemistry, Genetics, and Medical Applications. Elsevier, New York.
2. Sharma, V, A. Jaishankar, Y.C. Wang, and G.H. McKinley. 2011. Rheology of Globular Proteins: Apparent Yield Stress and Interfacial Viscoelasticity of Bovine Serum Albumin Solutions. Soft Matter. 7**:**5150-5160
3. Brownsey, G.J., T.R. Noel, R. Parker, and S.G. Ring. 2003. The Glass Transition Behavior of the Globular Protein Bovine Serum Albumin. Biophys. J. 85:3943-3950.
4. Tanford, C., and J.G. Buzzell. 1956. The Viscosity of Aqueous Solutions of Bovine Serum Albumin between pH 4.3 and 10.5. J. Phys. Chem. 60:225-231.
5. Tanford, C, J.G. Buzzell, D.G. Rands, and S.A. Swanson. 1995. The Reversible Expansion of Bovine Serum Albumin in Acid Solutions. J. Phys. Chem. 77:6421-6427.
6. Saluja, A., and D.S. Kalonia. 2005. Application of Ultrasonic Shear Rheometer to Characterize Rheological Properties of High Protein Concentration Solutions at Microliter Volume. J. Pharm. Sci. 94:1161-1168.
7. Gaigalas, A.K., V. Reipa, J.B. Hubbard, J. Edwards, and J. Douglas. 1995. A Non-Perturbative Relation between The Mutual Diffusion Coefficient, Suspension Viscosity, and Osmotic Compressibility: Application to Concentrated Protein Solutions. Chem. Eng. Sci. 50:1107-1114.
8. Monkos, K. 1996. Viscosity of Bovine Serum Albumin Aqueous Solutions as a Function of Temperature and Concentration. Int. J. Biol. Macromol. 18:61-68.
9. Sun, S.F. 1969. The pH Dependence of the Reduced Viscosity of Modified Serum Albumins. Arch. Biochem. Biophys. 129:411-415.
10. Lee, J., and A. Tripathi. 2005. Intrinsic Viscosity of Polymers and Biopolymers Measured by Microchip. Anal. Chem. 77:7137-7147.
11. Heinen, M., F. Zanini, F. Roosen-Runge, D. Fedunova, and F. Zhang, M. Hennig, T. Seydel, R. Schweins, M. Sztucki, M. Antalik, F. Schreiber, and G. Nägele. 2012. Viscosity and Diffusion: Crowding and Salt Effects in Protein Solutions. Soft Matter. 8:1404-1419.
12. Giordano, R., G. Maisano, F. Mallamace, N. Micali, and F. Wanderlingh. 1981. Structural Properties of Macromolecular Solutions. J. Chem. Phys., 75:4770-4775.
13. Jachimska, B., M. Wasilewska, and Z. Adamczyk. 2008. Characterization of Globular Protein Solutions by Dynamic Light Scattering, Electrophoretic Mobility, and Viscosity Measurements. Langmuir, 24:6866-6872.
14. Curvale, R., M. Masuelli, and A.P. Padilla. 2008. Int. J. Biol. Macromol., 42:133-137.
15. Yadav, S., S.J. Shire, and D.S. Kalonia. 2011. Viscosity Analysis of High Concentration Bovine Serum Albumin Aqueous Solutions. Pharm. Res. 28:1973-1983.
16. Oates, K.M.N., W.E. Krause, R.L. Jones, and R.H. Colby. 2006. Rheopexy of Synovial Fluid and Protein Aggregation. J.R. Soc. Interface 3:167-174.
17. Bloomfield, V. 1969. The Structure of Bovine Serum Albumin at Low pH. Biochem. 5:684-688.
18. Bowen, W.R., and P.M. Williams. 2001. Prediction of the Rate of Cross-flow Ultrafiltration of Colloids with Concentration-dependent Diffusion Coefficient and Viscosity – Theory and Experiment. Chem. Eng. Sci. 56:3083-3099.

19. Chikazumi, N., and T. Ohta.1991. Estimation of Hydrodynamic Volume of Proteins using High-performance Size-exclusion Chromatography and Intrinsic Viscosity Measurement: An Attempt at Universal Calibration. J. Liq. Chromat. 14:406-413

20. Ikeda, S., and K. Nishinari. 2001. On Solid-like Rheological Behaviors of Globular Protein Solutions. Food Hydrocoll. 15:401–406